PAPER

Check for updates

Formulation and evaluation of isosorbide dinitrate-loaded flash-release dispersible sublingual wafers

Shivakumar H. Nanjappa, [iD] *†[a,c] Vanita Somasekhar,†[b,c] Megha Kamath,[a,c] Sanjana S. Prakash,[a,c] Avichal Kumar,[a,c] Raksha Pai[b,c] and Rushikesh Shinde[a,c]

This study aimed to design flash-release dispersible sublingual wafers of isosorbide dinitrate (ISDN) by lyophilisation (LYO) by applying the principles of Quality by Design (QbD). Sublingual wafers and films were developed by LYO and solvent casting (SC) techniques, respectively, via a 2^3 factorial design using hydroxypropyl methylcellulose E15 as polymer and propylene glycol as plasticizer. Scanning electron microscopy (SEM) revealed the porous nature of these wafers with sub-micron-sized pores, while atomic force microscopy (AFM) indicated their homogeneous surface with minimal irregularities (<3.5 nm). Fourier transform infrared (FTIR) spectroscopy proved the chemical integrity of ISDN in the polymer matrix. Differential scanning calorimetry (DSC) and X-ray diffraction (XRD) conclusively indicated amorphisation of ISDN in the hydrophilic polymeric matrix in the wafers. Structural analysis was performed with a surface area and pore size analyser using liquid nitrogen as adsorbent and revealed that the wafers displayed significantly higher ($p < 0.05$) specific surface area (13.428 m^2 g^{-1}) and pore volume (~0.013 cc g^{-1}) values compared to the films. Density analysis by the gravimetric method further indicated that the density of the films (1.44 $\pm$ 0.23 g cm^{-3}) was found to be significantly higher ($p < 0.04$) than that of the wafers (0.633 $\pm$ 0.012 g cm^{-3}), confirming the denser microstructure of films and the porous nature of wafers. Wafers developed by optimising the LYO process displayed significantly shorter ($p < 0.0001$) disintegration time (3.1 $\pm$ 0.5 s) and time taken for 80% drug release (46 $\pm$ 0.2 s), compared to films produced by the SC technique. ISDN sublingual wafers exhibited a transmucosal flux that was comparable ($p > 0.05$) to that from the drug solution, indicating the potential to elicit a quick onset. The sublingual wafers that were found to rapidly disperse and quickly dissolve are likely to evade first-pass metabolism and elicit a prompt onset. The studies indicate that the developed sublingual wafers will be a promising platform for prophylactic management of cardiac emergencies.

Introduction

Cardiovascular diseases have been responsible for approximately one-third of deaths globally. Among cardiovascular illnesses, ischemic heart disease (IHD) is reported to be the most prevalent.[1] IHD is known to manifest as myocardial infarction and ischemic cardiomyopathy. The incidence of IHD is expected to increase in the coming years due to the increased prevalence of obesity, diabetes, metabolic syndrome, and an ageing population. Rapid urbanisation and globalisation in lower and middle-income countries have led to increased deaths and disabilities due to IHD. Isosorbide dinitrate (ISDN) is one of the drugs of choice prescribed to manage symptoms of angina, coronary heart disease, and heart failure.[2] The drug stimulates the soluble intracellular enzyme guanylyl cyclase, which upregulates the levels of cyclic guanosine 3′,5′-monophosphate (cGMP). The increase in cGMP activates cGMP-dependent protein kinase, causing vasorelaxation by phosphorylating proteins that regulate the uptake of calcium into cells.[3] ISDN is known to play a unique anti-anginal role, mediating nitric oxide release when administered orally. The drug has been employed in prophylactic management of IHD, especially with those with unstable angina, acute myocardial infarction, and heart failure.[4] Acute administration of ISDN is crucial to elicit a quick onset that could offer timely protection against angina pectoris, chronic heart failure, and pulmonary congestion. However, on oral administration, ISDN exhibits a short half-life (45 min), peak concen-

[a]*Department of Pharmaceutics, KLE College of Pharmacy, Bengaluru, India.*
E-mail: shivakumarhn@gmail.com
[b]*Department of Pharmaceutical Analysis, KLE College of Pharmacy, Bengaluru, India*
[c]*KLE Academy of Higher Education and Research, Belagavi-590010, Karnataka, India*
† Equal first author.

trations (6 min), and a short duration of action lasting for 10 to 60 min.[5] In addition, the drug is known to exhibit poor oral bioavailability (22–29%) as it is prone to extensive first-pass metabolism in the liver and enzymatic degradation in the gastrointestinal tract. Moreover, oral administration would be quite challenging for those patients who have lost consciousness during an angina attack. Therefore, sublingual ISDN administration would be preferred *via* a prophylactic, as this approach is known to overcome the first-pass effect and has the ability to elicit a rapid response to offer timely protection against angina. ISDN is known to be the most preferred nitrate as it quickly relieves pain in angina sufferers within minutes of its sublingual dosing. Considering the urgent clinical need to elicit a quicker onset and mitigate extensive first-pass metabolism, fast-disintegrating tablets,[6] orodispersible films,[7] and sublingual strips[8] have been developed. In this context, the present investigation aims to develop and evaluate novel flash-release sublingual dispersible wafers using the freeze-drying process. Lyophilisation (LYO) involves lowering the temperature of the solution by deep freezing to a temperature ranging from −50 to −80 °C followed by freeze-drying the frozen gel under reduced pressure. The vaporisation of frozen drug-loaded material is facilitated by a gradual increase in temperature during the process. The fast-melting tablets developed by this technology are known to disintegrate and dissolve rapidly when inserted under the tongue.[9]

Wafers are thin polymeric strips having a thickness of less than 500 μm that can dissolve within seconds at the site of insertion.[10] The wafers have proved to be a vital drug delivery platform in prophylactic management of angina pectoris, as they can be easily inserted into the sublingual region without the need for water once the patient is able to sense the signs of cardiac distress. On insertion, the high mucosal vasculature will enable quicker onset and improved transmucosal absorption that can evade the pathological manifestations arising from cardiac ischemia. In this context, the present investigation aims to develop fast-dissolving wafers of ISDN employing Design of Experiments (DoE). DoE is an integral and essential tool employed within the broader framework of Quality by Design (QbD). QbD aims to build quality in the product during pharmaceutical development. Therefore, we plan to elucidate the effects of these parameters. These include the processing method, volume of casting solution, and surface area of casting plates on the Critical Quality Attributes (CQAs) of the wafers, namely the disintegration time (DT) and time taken for 80% of the drug to be released ($t_{80\%}$). The other focus of the current investigations was to validate the mathematical models generated by optimising the process parameters in view of developing a wafer formulation with the most desirable CQAs. The proposed lyophilised wafer that will be able to quickly release ISDN to mitigate cardiovascular emergencies is a novel and first-of-its-kind development, as no such investigations have been reported for ISDN to date, to the best of our knowledge.

Materials and methods

Materials

ISDN was procured from Yarrow Chem Products Pvt. Ltd, Mumbai, India. Hydroxypropyl methylcellulose (HPMC) E15, sodium starch glycolate (SSG), propylene glycol (PG), and citric acid (CA) were obtained from S.D. Fine Chemicals, Mumbai, India. Mannitol was supplied by FMC (India) Pvt. Ltd. All chemicals and excipients used were of analytical or pharmacopeial grade and used as received without further purification.
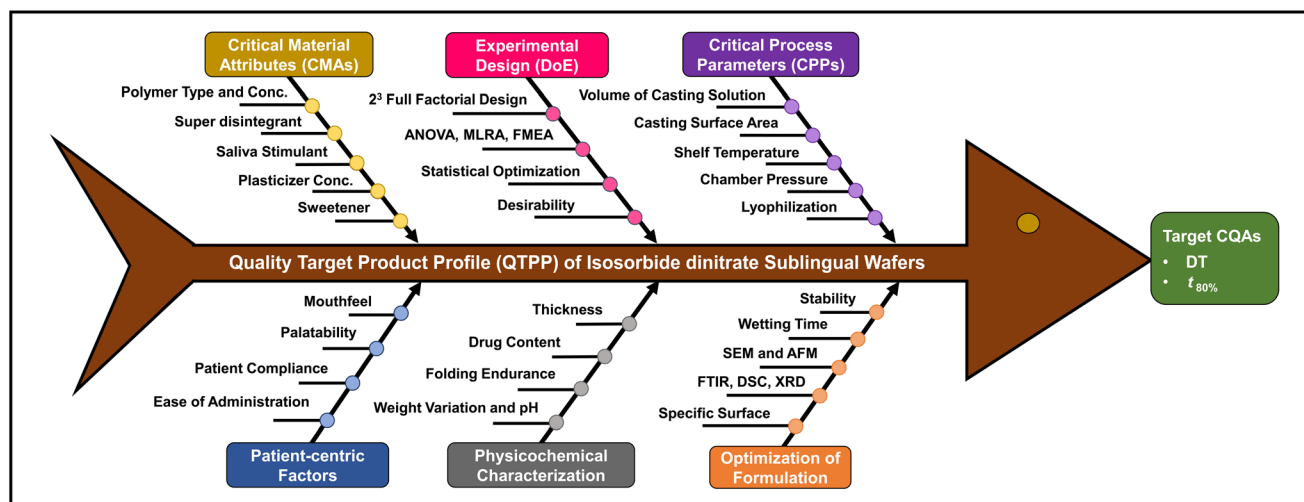
Preparation of the sublingual wafer of isosorbide dinitrate

Sublingual films and dispersible wafers of ISDN were developed *via* a conventional solvent casting technique (SC) and lyophilisation, respectively, using HPMC E15 as the polymer and propylene glycol (PG) as the plasticiser.[11] The composition of the casting solution was optimised after undertaking a series of preliminary trials. Failure Mode and Effect Analysis (FMEA) was employed to identify critical process parameters that would significantly influence the CQAs of the final product (Fig. 1). The integration of QbD with FMEA in our study provides a robust framework for formulation development. QbD systematically builds quality into the product by identifying critical parameters, while FMEA proactively assesses and prioritizes potential failure modes and risks. This combined approach enhances process understanding, reduces variability, and ensures a more reliable and efficient development pathway. It supports risk-based decision making and strengthens control strategies, ultimately leading to safer and higher-quality pharmaceutical products.

An eight-trial 2^3 factorial design with three variables that were varied across two levels was set up in Design Expert® version 13 to optimise the processing parameters in order to produce the dispersible wafers with the most desirable features. The drying method was the first variable (X_1), while the area of the Petri plate used for casting was the second parameter (X_2), whereas the volume of the casting solution (X_3) loaded into each Petri plate was deployed as the third independent variable. The casting solution was prepared by sequentially dispersing the excipients in distilled water under sonication, followed by incorporation of ISDN until a clear solution was obtained. The composition of the casting solution was finalised to ISDN (0.2% w/w), HPMC E15 (2% w/w), propylene glycol (1% w/w), mannitol (0.2% w/w), SSG (1% w/w), and CA (1% w/w). The effect of the three critical variables on the key responses, such as DT (Y_1) and $t_{80\%}$ (Y_2), was systematically investigated. The factors and the corresponding levels have been listed in Table 1.

The independent variables employed during each trial to produce a total of eight batches of model formulations are listed in Table 2. For the four trials employing SC (runs 1, 2, 4, and 5), accurately measured volumes of casting solutions were carefully transferred into flat-bottom Petri plates placed on a horizontal platform under an inverted funnel. The tip of the funnel was covered with aluminium foil and subjected to drying at room temperature (RT). The other four trials (runs 3,

Fig. 1 Failure mode and effect analysis (FMEA), illustrating risk analysis for the development of isosorbide dinitrate sublingual wafers. MLRA: multi-linear regression analysis; ANOVA: analysis of variance; DT: disintegration time; and $t_{80\%}$: time taken for 80% drug release.

Table 1 Factors and the corresponding levels for the development of isosorbide dinitrate-loaded films and flash-release wafers by conventional solvent casting and lyophilisation techniques

Independent variables	Low level	High level
X_1: processing method	Lyo[a]	SC[b]
X_2: area of the Petri plate (cm^2)	44.16	66.44
X_3: volume of casting solution (mL)	6	12

Dependent variables		Constraints
Y_1: disintegration time (s)		Minimize
Y_2: time for 80% dissolution (s)		Minimize

[a] Lyophilisation. [b] Solvent casting.

Table 2 Model formulations of films and wafers produced by varying the process variables as per 2^3 factorial design

Run	Processing method	Area of Petri plate (cm^2)	Casting solution volume (mL)
1	SC[a]	66.44	12
2	SC[a]	66.44	6
3	LYO[b]	44.16	12
4	SC[a]	44.16	12
5	SC[a]	44.16	6
6	LYO[b]	44.16	6
7	LYO[b]	66.44	6
8	LYO[b]	66.44	12

[a] Solvent casting (SC) resulted in film. [b] Lyophilisation (LYO) resulted in the formation of wafers.

6, 7, and 8) involved casting the solutions in Petri plates that were subsequently deep frozen for 24 h (ULT Freezer, Inkarp Instruments, India). After freezing, the frozen gels were loaded into a lyophiliser (Alpha 1–2 LD Plus, Martin Christ, Germany) and dried at a temperature of −50 °C and a pressure of 0.028 mbars for a period of 48 h to finally obtain the dispersi-

ble wafers (Fig. 2). The films and wafers thus obtained were stored in a desiccator before further characterization studies.

Regression analysis

The targeted responses that included DT and time taken for 80% release ($t_{80\%}$) were statistically analysed employing one-way analysis of variance (ANOVA) at a significance level of 0.05. The individual parameters were evaluated using the F test, and polynomial models, as represented in the form of eqn (1), were generated for each of the responses:

$$Y = \beta_1 X_1 + \beta_2 X_2 + \beta_3 X_3 + \beta_4 X_1 X_2 + \beta_5 X_2 X_3 + \beta_6 X_1 X_3 + \beta_7 X_1 X_2 X_3 \tag{1}$$

where Y stands for the measured response, β_1–β_7 are the regression coefficients, X_1, X_2, and X_3 are the three main effects, while $X_1 X_2$, $X_2 X_3$, and $X_1 X_3$ represent the two-way interactions, whereas the term $X_1 X_2 X_3$ would be the three-way interaction. A backward elimination approach was employed to eliminate the insignificant terms and refine the mathematical models so as to include only the significant terms. Fit analysis was performed to compare experimental values with those predicted by the mathematical models. The models generated by regression analysis were used to construct the three-dimensional plots. Furthermore, the effects of each of the critical terms on the response parameters were analysed using the contour plots and box plots.

Optimisation of the process parameters

The study aimed to optimise the process parameters in order to formulate wafers with optimal CQAs, such as short DT and $t_{80\%}$, which are vital to ensure prompt prophylactic protection in cardiac emergencies. In order to validate the models and thereby optimise the process parameters and establish a design space, a new wafer formulation that differed in compo-
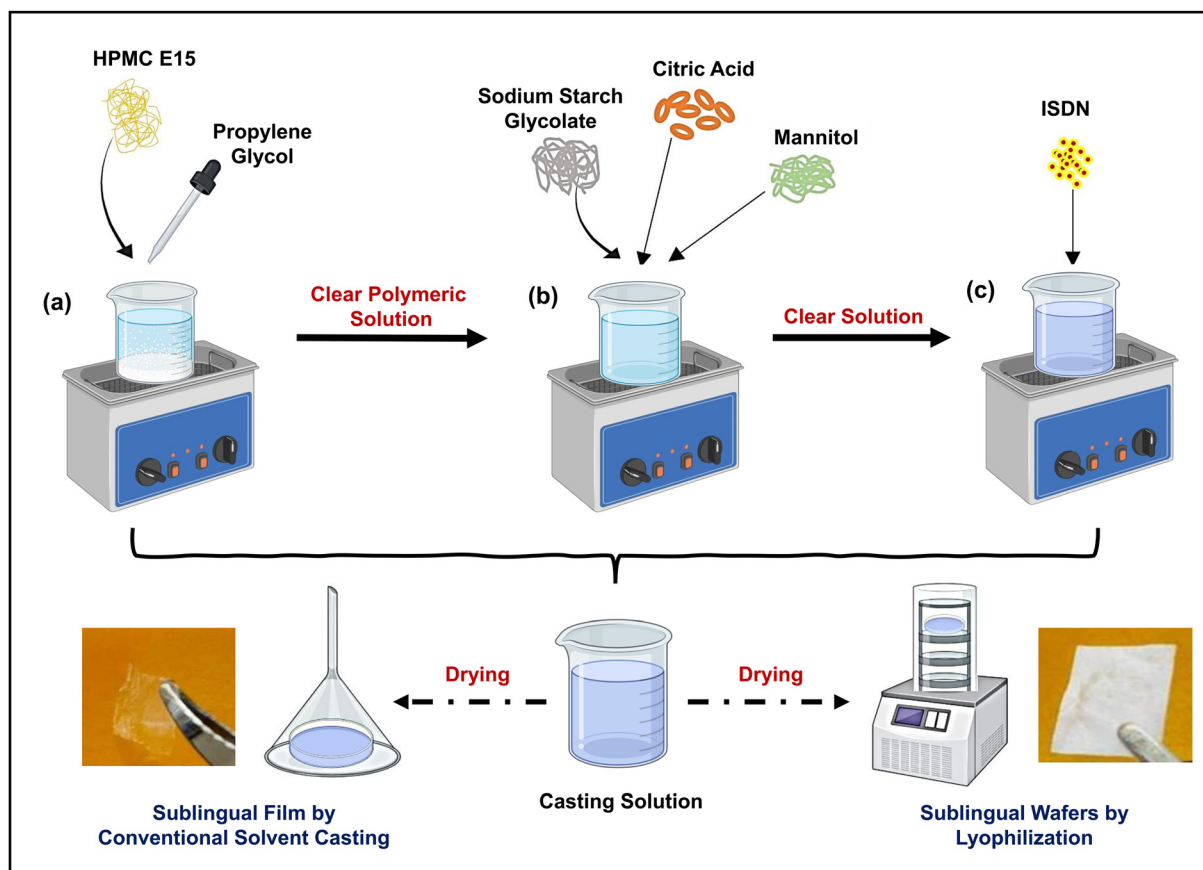
Fig. 2 Schematic representation of the formulation process of isosorbide dinitrate-loaded sublingual systems, including casting solution preparation (a–c) and subsequent drying steps to obtain sublingual films and wafers.

sition from the model formulations was developed. A numerical optimisation approach utilising the desirability approach was employed to determine the optimal settings for developing the new wafer formulation. The new wafer formulation with optimal CQAs was developed by lyophilisation on setting constraints to minimise DT and $t_{80\%}$ (Table 1). Feasibility studies and grid searches were executed to optimise the process parameters in order to develop a new wafer formulation with the most desirable CQAs. The new formulations developed were evaluated to acquire the experimental data before comparison with that predicted by the mathematical models generated to deduce the prediction error.

Evaluation of sublingual formulations

The films and wafer samples were subjected to various physicochemical evaluations, including weight variation, thickness, surface pH, porosity, DT, and *in vitro* dissolution.

Weight variation. Weight variation was evaluated by cutting 1×1 cm^2 pieces from three distinct areas of the samples and measuring their weight with an electronic analytical balance (Shimadzu BL-220H, Kyoto, Japan). The average weight of the samples was calculated before presenting the results as the mean ± standard deviation (S.D.) based on three measurements.[12]

Thickness. The thickness of the samples was determined using a digital vernier calliper (Mitutoyo 500-196-30 Digital Calliper, Kawasaki, Japan). Three different points on each sample were used to assess the uniformity in thickness, and results were expressed as mean ± S.D.[13]

Folding endurance. The folding endurance (FE) of the samples was evaluated by repeatedly folding each sample at the same spot until it fractured. The FE was determined by recording the number of folds made at the same spot before the sample breaks. The FE was determined for three different samples of each formulation, and the results were reported as mean ± S.D.[14]

Surface pH. Surface pH is a crucial factor that determines the tendency of the sample to cause irritation on sublingual application. The pH of the samples was measured by placing them in a Petri dish with 0.5 mL of phosphate buffered saline (PBS, pH 6.8). The sample was immersed and allowed to equilibrate in PBS for approximately 40 s. After equilibration, the electrode of a pH meter was brought into contact with the surface of the sample to determine the pH in triplicate using a digital pH meter (Digisun Electronics, Hyderabad) at 37 ± 2 °C.[12]

Disintegration time. The rate at which the drug is released from the samples depends on the time it takes to disintegrate.

The DT of ISDN-loaded formulations was assessed in a Petri dish containing PBS buffer (pH 6.8). The Petri dish was placed on the hot plate of a magnetic stirrer (Remi, 1-MLH, Mumbai) set to 50 rpm, and the temperature was maintained at around 37 ± 0.5 °C. The time taken for the samples to fragment into pieces was noted as the DT and was reported as the mean $\pm$ S.D. of three determinations.[15]

Drug content. The amount of ISDN in the samples was determined by dissolving the samples in ethanol. The 1×1 cm^2 film pieces were dissolved in 10 mL of ethanol and subjected to sonication.[16] The resulting solution was filtered through a 0.45 µm Whatman filter paper. The filtrate was suitably diluted with phosphate buffer (pH 6.8) in a volumetric flask. The assay of the different model formulations was determined by employing the slope of the standard calibration curve generated in triplicate by ultra-fast liquid chromatography (UFLC).[17]

In vitro dissolution studies. The *in vitro* dissolution of the samples was carried out using USP dissolution apparatus type-V (Electrolab TDT-08L, Mumbai) with 200 mL of pH 6.8 PBS as the dissolution medium, maintained at 37 ± 0.5 °C. The samples were affixed on the disc using a clamp and placed under the paddle with the dissolution medium agitated at 50 rpm during the study.[11] The withdrawn samples were suitably diluted and analysed at a detection wavelength of 210 nm and a run time of 10 min by UFLC.[18] Furthermore, the percentage dissolution efficiency (%DE) was calculated based on the area under the drug release profile curve (eqn (2)). Higher values of %DE indicate the potential of the formulation to generate a pulsatile or a flash drug release:

$$\%\text{DE} = \frac{\int_{t_0}^{t} y_t(\mathrm{d}t)}{y_{100} \times t} \times 100 \tag{2}$$

where 't_0' is the initial and 't' is the final time point of the dissolution study, 'y_t' is the percentage of drug dissolved at any time 't', and 'y_{100}' is 100% dissolution (maximum dissolution).

Characterisation of optimised wafers

Drug-excipient compatibility analysis. Drug–polymer compatibility was assessed using a Fourier transform infrared (FTIR) spectrophotometer (Jasco 450 Plus spectrophotometer, ECC 450, Easton, MD, USA). The FTIR spectra of ISDN, the physical mixture, and the samples were recorded by mixing the samples thoroughly with potassium bromide in a glass mortar. The resulting samples were then loaded into an IR diffuse reflectance sampler and exposed to infrared radiation before scanning in the range of 4000 and 1000 cm^{-1} to record the IR spectra.[19]

Differential scanning calorimetry. Differential Scanning Calorimetry (DSC) is employed to evaluate the solid state of ISDN in the formulations. Thermal analysis of ISDN, the physical mixture, and the optimised wafer was performed using a differential scanning calorimeter (DSC-60-Shimadzu, Tokyo, Japan). About 10 mg of each sample was transferred to a sealed aluminium container and heated gradually at a rate of

10 °C min^{-1} in the temperature range of 30–130 °C while purging with nitrogen (50 mL min^{-1}). The degree of crystallinity (X_c) of the sample was calculated relative to ISDN using eqn (3):[20]

$$X_c = \frac{\Delta H}{(1 - w) \cdot \Delta H^\circ} \tag{3}$$

where ΔH is the experimental heat of fusion of the sample, ΔH° is the heat of fusion of crystalline ISDN, and w is the weight fraction of ISDN in the sample.

X-ray powder diffraction. The XRD patterns were determined using a Bruker D8 Advance X-ray diffractometer, which has a 2.2 kW Cu anode X-ray source and a fine-focus ceramic X-ray tube, operating at 40 kV and 40 mA with a total power of 1.6 kW. Crystallinity of the samples was assessed by comparing the peak heights in the diffractograms of the samples relative to ISDN, used as a reference. The relative degree of crystallinity (RDC) was computed using eqn (4):[20]

$$\text{RDC} = \frac{I_{\text{sample}}}{I_{\text{refer}}} \times 100 \tag{4}$$

where, I_{refer} is the intensity of the reference characteristic peak of ISDN, while I_{sample} is the intensity of the sample peak at the same 2θ values as the reference.

Morphological and surface topographical analysis. Scanning electron microscopy (SEM) and bright field microscopy were utilized to analyse the surface morphology and topographical features of the samples. SEM images under appropriate resolution were acquired using a scanning electron microscope (Tescan Vega 3, Brno, Czech Republic). The samples were mounted on double-sided adhesive tape and then coated with approximately 200 nm of gold under a reduced pressure of 0.0133 Pa. This process was carried out for 5 min using an ion sputtering device set to a voltage of 10 kV.[21] In addition, a trinocular research microscope (Model: BX 53, Olympus, Germany) was used to study the surface morphology of the samples. The samples were placed on a glass plate and illuminated under a bright light source.[22]

Atomic force microscopy. Atomic force microscopy (AFM) was utilised to capture high-resolution 3D images of wafers containing ISDN. The surface roughness parameters R_a, R_q, and R_z of ISDN wafers were assessed with AFM (Innova SPM Atomic Force Microscope, USA). Surface roughness (R_a) is the arithmetic average of the absolute values of surface height deviations from the mean plane, while root mean square roughness (R_q) represents the SD of the height values within the examined area whereas maximum surface profile height (R_z) measures the average vertical distance between the highest peaks and lowest valleys relative to the mean plane.[23]

Structural characterisation. The pore structure characterization of films and wafers of ISDN was performed using liquid nitrogen as an adsorbent in a Nova Station v11.05 high-speed surface area and pore size analyzer (Quantachrome Instruments). The surface area was calculated by the gas adsorption method following the standard Brunauer–Emmett–Teller (BET) method, and the pore diameter and pore volume

were determined from adsorption isotherms using the Barrett–Joyner–Halenda (BJH) method.[24] The density of the ISDN films and wafers was determined by the gravimetric method reported in the literature.[25]

Wetting time. Wetting times were assessed by determining the time required for samples to completely take up water and wet the whole surface. Whatman filter paper measuring 5.5 cm in diameter was placed on Petri plates. About 10 mL of a solution of methyl orange maintained at a temperature of 37 ± 0.5 °C was added to the plate. The time taken for the samples placed on the filter paper to become wet was recorded in triplicate and averaged to obtain the wetting time.[26]

***Ex vivo* permeation studies.** *Ex vivo* permeation studies were performed using a Franz diffusion cell (Orchid Scientific, India). The receptor chamber was filled with freshly prepared simulated salivary fluid (SSF), while fresh porcine buccal mucosa was mounted between donor and receptor compartments with the epithelial side facing the donor chamber. The wafer was placed on the donor chamber while the SSF in the receptor was maintained at 37 ± 2 °C under magnetic stirring at 600 rpm. Samples were withdrawn every 10 min over 1 h, filtered through a 0.45 μm membrane, and replaced with equal volumes of fresh medium. The drug concentration was determined by UFLC, and the amount of ISDN permeated was calculated using a calibration curve in SSF.[18] The steady state flux was deduced from the slope of the linear portion of the plot of the amount of ISDN permeated per cm^2 on the Y axis *versus* time on the X axis.

Stability studies. The optimised ISDN wafers were first evaluated for different parameters, then wrapped in butter paper and kept in aluminium pouches at RT for 3 months. After storage, the percentage drug content (DC), FE, DT, moisture loss of the wafers, and $t_{80\%}$ were assessed at 1, 2, and 3 months and compared to the results obtained before the storage period.[11]

Analytical method

The samples generated during the studies were analysed by a UFLC system (Prominence, Shimadzu Analytical Pvt. Ltd) equipped with a UV-visible detector (SPD-20A) and a manual injector. The elution was carried out on an Intek Chromasol Coral C18 BDS column (150 mm × 4.6 mm, 5 μ, 130 Å). The mobile phase comprising a mixture of methanol and water in the ratio of 40 : 60 v/v was set to a flow rate of 1 mL min^{-1}. The samples measuring 20 μL were analysed at a detection wavelength of 210 nm and a run time of 10 min. The chromatogram of each of the samples was recorded using Lab Solutions software.

Statistical analysis

The experimental design was set up, and the results obtained were statistically analysed using Design-Expert® software version 13.0.5.0. A *p*-value of less than 0.05 was considered to be statistically significant. The statistical analysis of the data generated was performed using GraphPad Prism version 6.

Results and discussion

Sublingual wafers and films of ISDN will be the ideal drug delivery platform to meet the urgent clinical need in prophylactic management of cardiac emergencies, including angina pectoris. The formulations that disperse quickly are likely to facilitate rapid dissolution of the drug in saliva, generating a pulsed dose that can be quickly absorbed through the sublingual mucosa to elicit a faster onset of action and thereby offer timely protection against cardiac emergencies. In addition, these formulations help to overcome first-pass metabolism and substantially improve the bioavailability.[27]

Design of experiments

A 2^3 factorial design was employed to optimise the drying parameters in order to obtain sublingual films and wafers. Preliminary studies indicated that the drying technique (*A*), area of the casting plate (*B*), and casting solution volume (*C*) were found to be the critical factors influencing the quality attributes of the resulting formulations. The effects of these critical process parameters on CQAs of the final products, such as DT (Y_1) and $t_{80\%}$ (Y_2), were systematically analysed using ANOVA. Eight different formulations of ISDN, which included four films and four wafers, were produced by SC and lyophilisation, respectively, as per the design. Lyophilisation has been identified as an effective drying technique to produce potential quick-acting, fast-dissolving wafers.[28] In addition, freeze drying enhances product stability, extends product shelf life, and allows storage at RT.[29] An ideal lyophilisation process has the potential to retain the original physical and chemical integrity of the product, achieve minimal residual moisture, and ensure long-term stability.[30] During lyophilisation, sublimation of the resulting ice under highly reduced pressure results in a highly porous three-dimensional structure.[31]

The composition of the casting solution remained unchanged across all experiments performed. HPMC E-15 was employed as the hydrophilic polymeric carrier, while SSG was used as the superdisintegrant. Low molecular weight HPMC is widely utilised in the development of orodispersible films and wafers.[32] HPMC E-15 is generally preferred for producing wafers because its low cross-linking density enables quick disintegration and instantaneous release of the contents.[33] SSG is a chemically modified and cross-linked starch commonly employed as a superdisintegrant in sublingual films.[11] Carboxymethyl substitution on specific hydroxyl groups improves water penetration, while the degree of cross-linking determines swelling and lowers polymer viscosity.[34] PG was used as a plasticiser, while mannitol served as the sweetener. With two hydroxyl groups per molecule, PG increases hydration, resulting in improved flexibility due to its plasticising effect.[35] Mannitol plays a vital role as a sweetener that exhibits good stability in dilute acid or alkali solutions and is resistant to oxidation when exposed to air.[36] Citric acid was used as a saliva-stimulating agent, as it can stimulate the sali-

Table 3 Physicochemical parameters of the isosorbide dinitrate sublingual films and wafers

Run	Technique (X_1)	Weight (mg)	Thickness (mm)	FE[c]	Surface pH	Moisture loss (%)	DC[d] (%)	DT[e] (s)	$t_{80\%}$[f] (s)
1	SC[a]	0.089 ± 0.05	0.08 ± 0.006	80 ± 1	6.24 ± 0.8	0.51 ± 0.05	95.30 ± 1.23	20.12 ± 0.1	330 ± 0.1
2	SC[a]	0.090 ± 0.05	0.07 ± 0.002	73 ± 5	6.31 ± 0.1	0.51 ± 0.07	95.12 ± 1.32	19.80 ± 0.5	260 ± 0.5
3	LYO[b]	0.082 ± 0.02	0.18 ± 0.001	267 ± 5	6.23 ± 0.1	0.52 ± 0.01	97.23 ± 1.34	4.31 ± 0.2	66 ± 0.2
4	SC[a]	0.087 ± 0.09	0.12 ± 0.001	76 ± 5	6.54 ± 0.3	0.53 ± 0.02	94.72 ± 1.54	22.12 ± 0.3	430 ± 0.1
5	SC[a]	0.086 ± 0.05	0.10 ± 0.003	72 ± 3	6.73 ± 0.2	0.61 ± 0.01	95.80 ± 1.62	21.20 ± 0.4	378 ± 0.2
6	LYO[b]	0.081 ± 0.07	0.11 ± 0.004	256 ± 2	6.76 ± 0.7	0.63 ± 0.06	96.12 ± 1.52	3.21 ± 0.8	53 ± 0.1
7	LYO[b]	0.083 ± 0.04	0.10 ± 0.003	280 ± 3	6.71 ± 0.5	0.53 ± 0.07	99.79 ± 1.68	2.20 ± 0.5	42 ± 0.3
8	LYO[b]	0.086 ± 0.02	0.09 ± 0.002	279 ± 1	6.80 ± 0.3	0.64 ± 0.06	94.57 ± 1.78	3.12 ± 0.2	29 ± 0.4

All data are expressed as mean ± SD ($n = 3$). [a] Solvent casting resulted in films. [b] Lyophilisation resulted in wafers. [c] Folding endurance. [d] Drug content. [e] Disintegration time. [f] Time taken for 80% drug release.

vary gland and thereby indirectly promote dissolution of drugs in the sublingual region of the oral cavity.[33]

Physicochemical characterisation of formulations

The physicochemical properties of the sublingual films and wafers are captured in Table 3. The average weight of the films and wafers measuring 1×1 cm^2 was found to range from 0.086 ± 0.05 mg to 0.090 ± 0.05 mg and from 0.081 ± 0.07 mg to 0.086 ± 0.02 mg, respectively. The consistent weight of the formulations suggests that the LYO, as well as SC, were able to produce wafers and films that had consistent weight.[37] Weight variation can directly influence the content uniformity of each formulation, which will be crucial in ensuring dose precision of potent medications like ISDN.

The average thickness of the sublingual films was found to range from 0.07 ± 0.002 to 0.12 ± 0.001 mm, while that of the wafers varied between 0.10 ± 0.003 and 0.18 ± 0.001 mm, respectively. The relatively higher thickness of the wafers can be attributed to the porous nature of the wafers compared to the denser films. The production of wafers by sublimation of the frozen polymeric gels under reduced pressure will eventually result in thicker, relatively porous wafers compared to the relatively thin and dense films that were produced by the SC technique.[31] A thickness of less than 1 mm was reported in the earlier literature for the esomeprazole sublingual wafers produced by a conventional solvent casting technique.[11]

The relatively greater thickness of the wafers can be attributed to the porous nature of the wafers compared to the denser films. The production of wafers by sublimation of the frozen polymeric gels under reduced pressure eventually results in thicker, relatively porous wafers compared to the relatively thin and denser films that were produced by the SC technique.[31] A thickness of less than 1 mm was reported in the earlier literature for the esomeprazole sublingual wafers produced by a conventional solvent casting technique.[11]

The FE studies revealed that the wafers produced were elastic and exhibited strong mechanical properties. The FE values for the films and wafers were found to range from 72 ± 3 to 80 ± 1 and 256 ± 2 to 280 ± 3, respectively. The superior physico-mechanical properties of the wafers justified the choice of the hydrophilic polymer used for the fabrication of

orodispersible formulations. PG served as a plasticiser, enhancing the elasticity of the wafers, positively imparting high FE. PG is known to reduce the stiffness of the polymer matrix, which helps prevent brittleness and breakage.[35] Plasticisers like PG are known to reduce the glass transition temperature to impart flexibility to films and wafers.[38,39]

Impact of process parameters on disintegration time

The mathematical model to illustrate the influence of different independent variables on DT is represented by eqn (5):

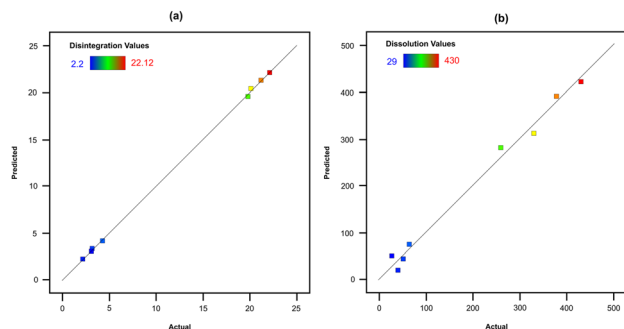$$Y_1 = 12.01 - 8.80A - 0.700B + 0.4075C + 0.1500AB \quad (5)$$

The F-value of the model was found to be 2691.42, indicating the equation generated for DT was statistically significant ($p <$ 0.0001). The Fisher F test revealed a very low probability value ($p_{model} > F$ less than 0.0001), which indicated the predictor model generated was highly significant. The value of the determination coefficient (predicted $R^2 = 0.9980$) was found to be in reasonable agreement with the adjusted determination coefficient (adjusted $R^2 = 0.9993$), indicating insignificant ($p > 0.05$) lack-of-fit of the model (Table 4). The actual values were found to be in close agreement with the predicted values, indicating that the model exhibits a good fit with no significant deviation between experimental and predicted responses (Fig. 3a).

The DT of the films was found to range from 19.80 ± 0.51 to 22.12 ± 0.3 s, while the DT varied from 2.20 ± 0.5 to 4.31 ± 0.2 s for the wafers. The drying process used was found to emerge as the most significant factor affecting the DT. The average DT of wafers was found to be significantly lower ($p < 0.0001$) compared to the DT of the films produced. The model indicates the overwhelming influence ($p < 0.0001$) of the drying process (A) employed on DT. Furthermore, the DT was found to be negatively affected by the drying surface area (B), although the effect was relatively less influential ($p < 0.003$). The drop in the

Table 4 Results of regression analysis and polynomial coefficients for each critical parameter attribute

Responses	F-Value	p-Value	Predicted R^2	Adjusted R^2
Y_1	2691.42	<0.0001	0.9980	0.9993
Y_2	6557.73	<0.0001	0.9997	0.9992

Fig. 3 Correlation plots of actual *versus* predicted values for the dependent variables: (a) disintegration time and (b) time to 80% drug dissolution ($t_{80\%}$). Each point represents an experimental run, and proximity to the diagonal line indicates strong agreement between experimental and model-predicted results.

thickness of the formulation with an increase in the surface area could be the possible reason for the decrease in DT. On the other hand, factor C was found to have a positive impact on DT, though the effect was found to have the least effect ($p < 0.017$). The predominant influence of lyophilisation on the DT of the wafers was clearly evident from the Pareto chart, box plot, and 3D plots (Fig. 4).

The porous nature of the wafers will normally facilitate quick diffusion of the fluid into the tortuous microstructure of the wafers and enable quicker hydration of the hydrophilic groups in the polymer matrix, enabling rapid disintegration compared to the denser films.[31] Thus, when exposed to saliva, the wafers allow rapid fluid uptake that will facilitate the quick breakdown or disintegration of the wafers.[40] It is notable that the pores in wafers play a pivotal role in allowing the ingress of

fluids into the wafer structure, thereby expediting the process of disintegration.
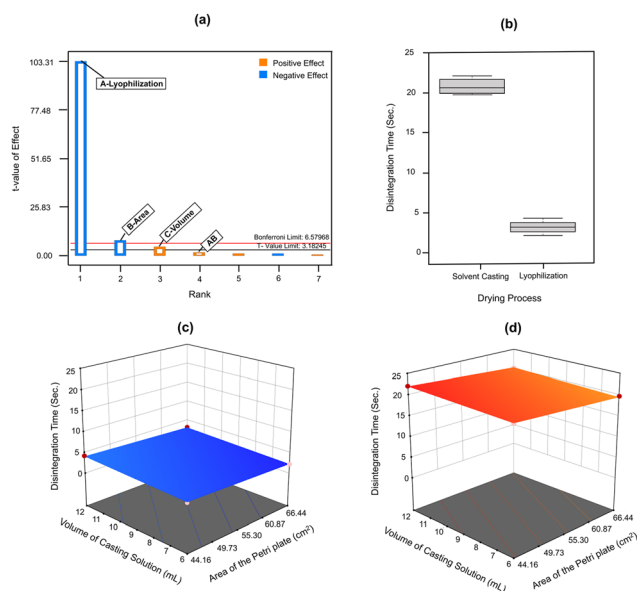
This porous nature substantially contributes to the rapid breakdown of the wafer upon contact with saliva in the sublingual cavity, which probably facilitates efficient drug absorption through the sublingual mucosa to elicit a rapid onset of action. The DT for wafers having a thickness of ~1 mm was reported to be within 30 s, which will result in accelerated drug dissolution as per the earlier literature.[11] Moreover, in the case of films, it was observed that the DT tends to increase proportionally with an increase in film thickness. The DT for films was found to be more than 20 s. This time was significantly higher ($p < 0.0001$) compared to that observed with wafers.

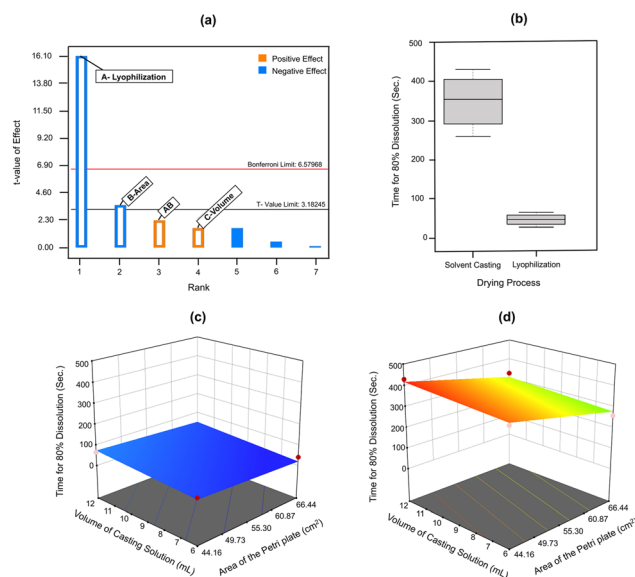### Impact of process parameters on dissolution

The mathematical model to illustrate the influence of different independent variables on $t_{80\%}$ is represented by eqn (6):

$$Y_2 = 198.50 - 151A - 33.25B + 15.25C + 21.25AB \quad (6)$$

The F-value of 6557.73 demonstrates strong statistical significance ($p < 0.0001$) of the mathematical model generated for $t_{80\%}$. The Fisher F test, yielding a very low probability value ($p_{model} > F$ value less than 0.0001), indicated the high level of statistical significance of the predictive model generated for $t_{80\%}$. The value of the determination coefficient (predicted $R^2 = 0.9992$) was in good agreement with the adjusted determination coefficient (adjusted $R^2 = 0.9997$), as the difference was less than 0.2, which highlights the lack-of-fit of the model was insignificant ($p > 0.05$). The actual values were found to be in close agreement with the predicted values, indicating that the

Fig. 4 Influence of lyophilisation depicted using a (a) Pareto chart, (b) box plot, and (c) 3D surface response, with comparison to (d) solvent casting on disintegration time.

Fig. 5 Influence of lyophilisation depicted using a (a) Pareto chart, (b) box plot, and (c) 3D surface response, with comparison to (d) solvent casting on time taken for 80% drug release.
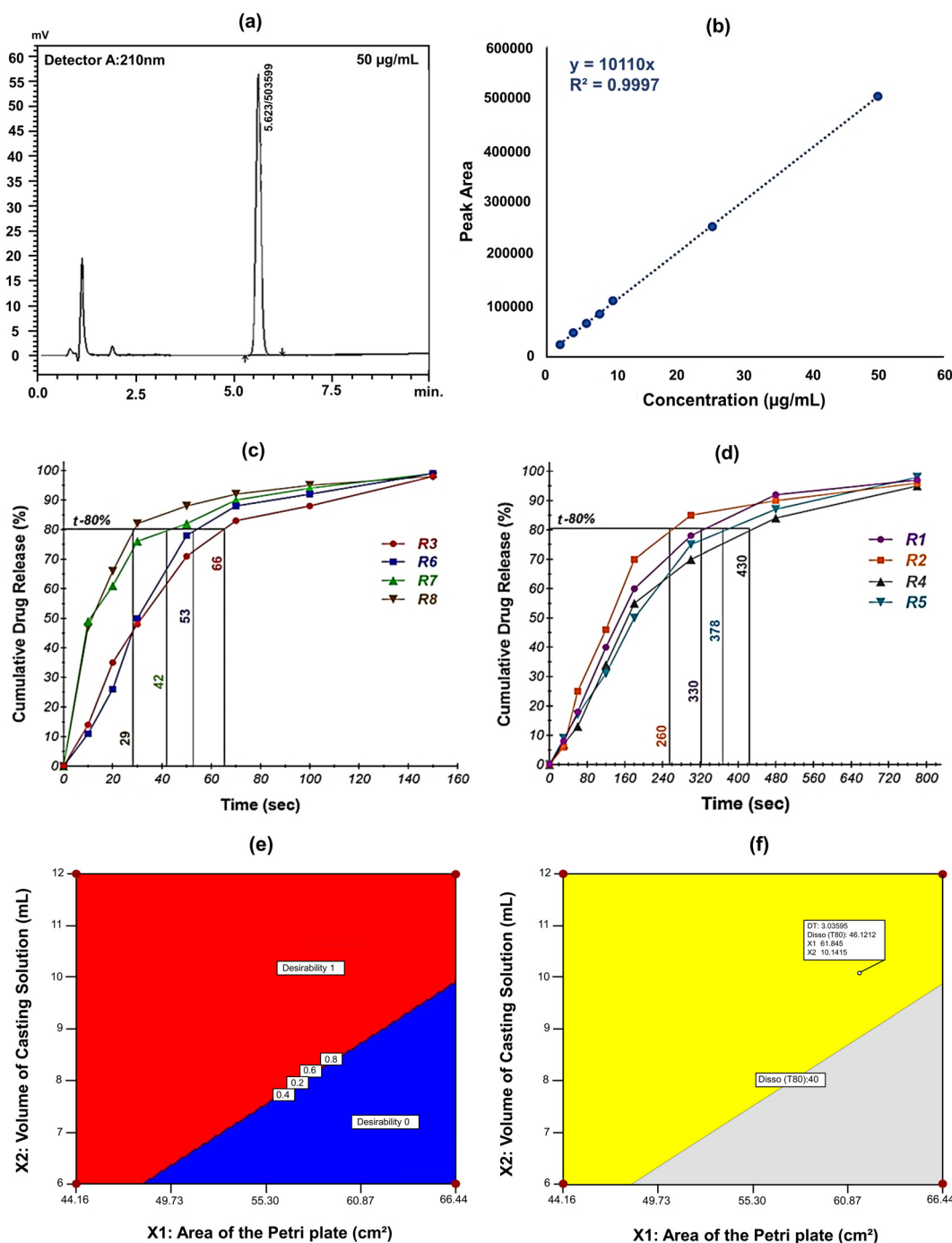
model exhibits a good fit with no significant deviation between experimental and predicted responses (Fig. 3b).

The dissolution was found to be dependent on factors A, B, with factor C having an insignificant effect. The ANOVA results indicated that A, B, and AB with $p < 0.0001$ had a positive effect on *in vitro* drug release (Table 4). Factors A were found to have the most pronounced effect on the $t_{80\%}$ value, followed by

factor B, which in turn was followed by the interaction effect AB. The dominating effect of lyophilisation on $t_{80\%}$ of the wafers is quite evident in the Pareto chart, box plot, and 3D plots (Fig. 5).

The HPLC chromatogram plot confirms specificity with retention time (5.62 min) captured in Fig. 6a with the linearity plot as shown in Fig. 6b. The dissolution profiles of the wafers

Fig. 6 (a) HPLC chromatogram and (b) linearity plot of isosorbide dinitrate; dissolution profiles of lyophilised ISDN: (c) wafer and (d) film formulations. (e) Desirability plot indicating optimal values of casting solution volume and surface area. (f) Overlay plot indicating the design space (yellow) and the parameter settings for the development of an optimal batch of wafers by lyophilisation.

(Fig. 6c) and the films (Fig. 6d) of ISDN were also acquired. It was observed that 50% of the drug was released within 10–35 s from the wafer formulations, which was found to range from 94.88 ± 0.018% to 99.41 ± 0.015% inside a minute. However, for the films, 50% of the drug was released between 14 and 20 min, and at 30 min, the release varied between 83.19 ± 0.018% and 92.81 ± 0.018%. The mean $t_{80\%}$ values for wafers were found to be significantly lower ($p < 0.0025$) compared to the films produced. Disintegration is considered to be the rate-determining step in the dissolution of soluble therapeutic agents.[41] The porous microstructure of the wafer was found to play a vital role in fluid penetration, which accelerated disintegration, resulting in rapid dissolution.[11]

Optimisation of the formulation

The desirability approach is one of the common methods that can be employed to optimise the process parameters.

The prediction will be more reliable when the desirability value approaches 1.0. The desirability plot and overlay plot areas are depicted in Fig. 6e and f, respectively. The predicted and experimental values, along with the corresponding prediction error, are captured in Table 5. The prediction error for DT and $t_{80\%}$ of the optimised formulation was observed to be

−0.26 to 1.30. The low prediction error values confirmed the validity of the mathematical models and clearly highlighted the prognostic ability of the models generated by multilinear regression analysis (MLRA) and ANOVA. Furthermore, the % DE of the optimised sublingual wafer (83.5 ± 3.5%) was found to be significantly higher ($p < 0.002$) compared to the sublingual film (62.5 ± 2.5%) developed. The superior dissolution performance of the wafer can be attributed to the porous structure of the hydrophilic matrix generated during lyophilisation, considerably amplifying the surface area, which in turn enables faster disintegration and quicker dissolution.

The desirability plot (Fig. 6e), depicting the casting solution volume and the surface area, attains the maximum value of 1.0. (plot coloured with red indicating higher values of desirability, while blue indicates low desirability values). The overlay plot (Fig. 6f) displays the yellow area that represents the design space, with the selected point indicating the optimal settings of lyophilisation (10.14 mL of casting solution spread across an area of 61.85 cm^2) that could produce wafers with a DT of 3.06 s and $t_{80\%}$ (46.12%).

Characterisation of optimised wafer formulationDrug–polymer compatibility analysis. The FTIR spectrum for ISDN displayed prominent peaks at 2965.98, 1381.75, and 1066.44 cm^{-1} (Fig. 7a). The peak at 2965.98 cm^{-1} can be related to C–H stretching vibrations, and the peak at 1381.75 cm^{-1} corresponds to NO$_2$ stretching, while the peak at 1066.44 cm^{-1} can be assigned to C–C stretching. Earlier studies reported FTIR peaks of ISDN at 2932, 1622, and 1083 cm^{-1}, which authenticated the spectral data generated.[37] The presence of these characteristic peaks in the physical mixture confirmed the chemical integrity of ISDN in the mixture. Furthermore, the characteristic peaks of ISDN appeared at 2056.71, 1344.12, and 1093.44 cm^{-1} in wafers, further confirming the chemical integrity of ISDN in the wafers and ruling out the possibility of any chemical inter-

Table 5 Comparison of the experimental values of the response parameters/product quality attributes of wafer formulations developed employing optimal settings with predicted values
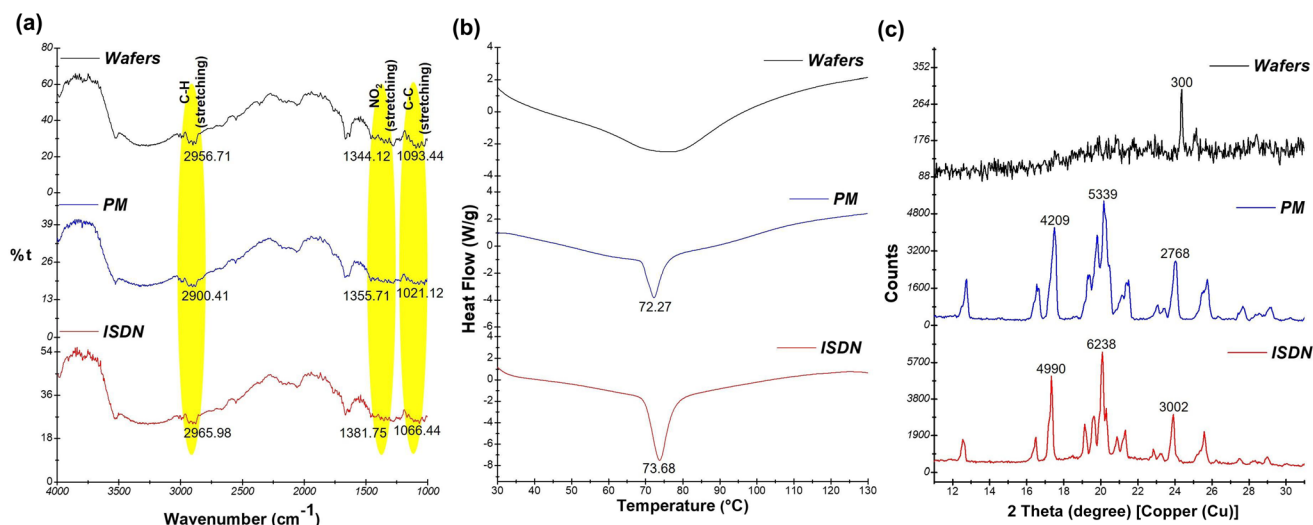
Optimal settings $A : B : C$	Response	Expt[b] value	Pred[c] value	Prediction error (%)
A: Lyo,[a] B: 61.85 cm^2, C: 10.14 mL	Y_1 (s)	3.1	3.06	1.30
	Y_2 (s)	46	46.12	−0.26

[a] Lyophilisation. [b] Experimental values. [c] Predicted values.

Fig. 7 Physicochemical characterisation of isosorbide dinitrate (ISDN), physical mixture (PM), and wafers: (a) FTIR spectra displaying characteristic peaks, (b) DSC thermograms, and (c) XRD patterns indicating crystallinity.
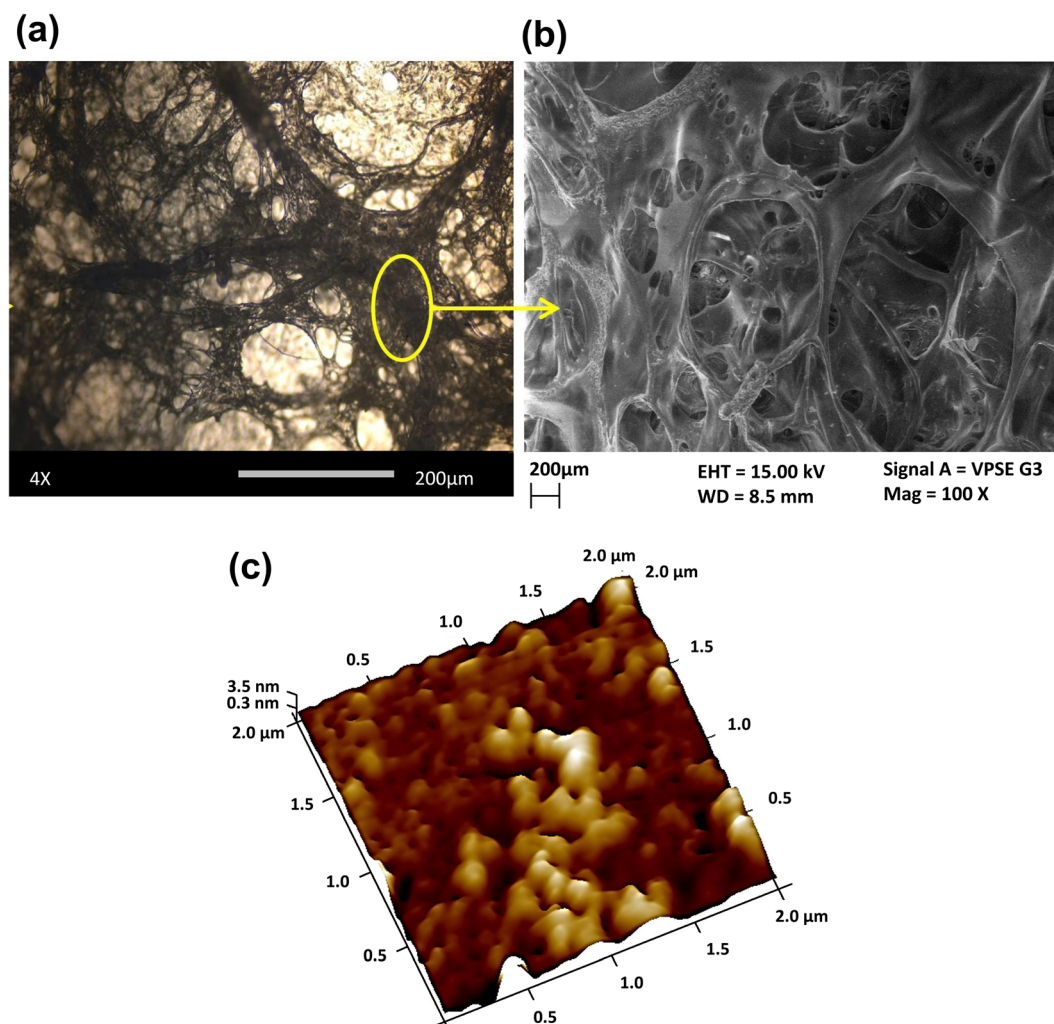
action between ISDN and excipients during the process of fabrication of wafers.[42]

Differential scanning calorimetry. The DSC scan revealed a prominent endothermic peak at 73.68 °C, with enthalpy of fusion (ΔH_f) of −96.14 J g^{-1}. These findings were found to match the melting transition temperature (72 °C) that was previously reported.[42] Likewise, the physical mixture also exhibited an endothermic peak at 72.27 °C, with reduced intensity (ΔH_f; −38.19 J g^{-1}), suggesting that nearly 79.41% of ISDN is likely dispersed in semicrystalline form in the mixture (Fig. 7b). The broad band devoid of any sharp peaks signifies that the drug is likely to be dispersed in an amorphous state in the hydrophilic polymer matrix.[43] The LYO process is known to render ISDN more amorphous in the polymer matrix during the fabrication process.

X-ray powder diffraction. The PXRD patterns revealed three prominent peaks at 2θ values of 17.3°, 20°, and 24° that displayed intensities of 4990, 6238, and 3002 counts, respectively, indicating the crystalline nature of ISDN (Fig. 7c). The peaks were in agreement with the reports as per the previous study, confirming the crystalline nature of the drug.[42] The diffractogram of the physical mixture displayed peaks at 17.3°, 20°, and 24° with intensities of 4209, 5339, and 2768 counts, respectively, indicating nearly 85% of ISDN existed in crystalline form. However, the diffractogram of wafers displayed only one characteristic low-intensity (300 counts) peak of ISDN at 24°, indicating a substantial drop in percentage crystallinity to nearly 9.9% of ISDN. These results collectively confirm the successful dispersion of ISDN into the wafer in a nearly amorphous form. The dispersion of ISDN in a nearly amorphous state in the hydrophilic matrix is likely to improve the drug dissolution, which in turn could generate a pulsatile release on contact with dissolution media or saliva.

Morphological and surface topographical analysis. Bright field microscopy revealed the distinctive morphology and topography of the wafers (Fig. 8a), while SEM images at low and high magnification (Fig. 8b) illustrated a porous polymeric network. Microstructural analysis showed uniformly distribu-

Fig. 8 Morphological characterisation of the wafers using (a) bright-field microscopy, (b) scanning electron microscopy, and (c) 3D topographic views by atomic force microscopy.
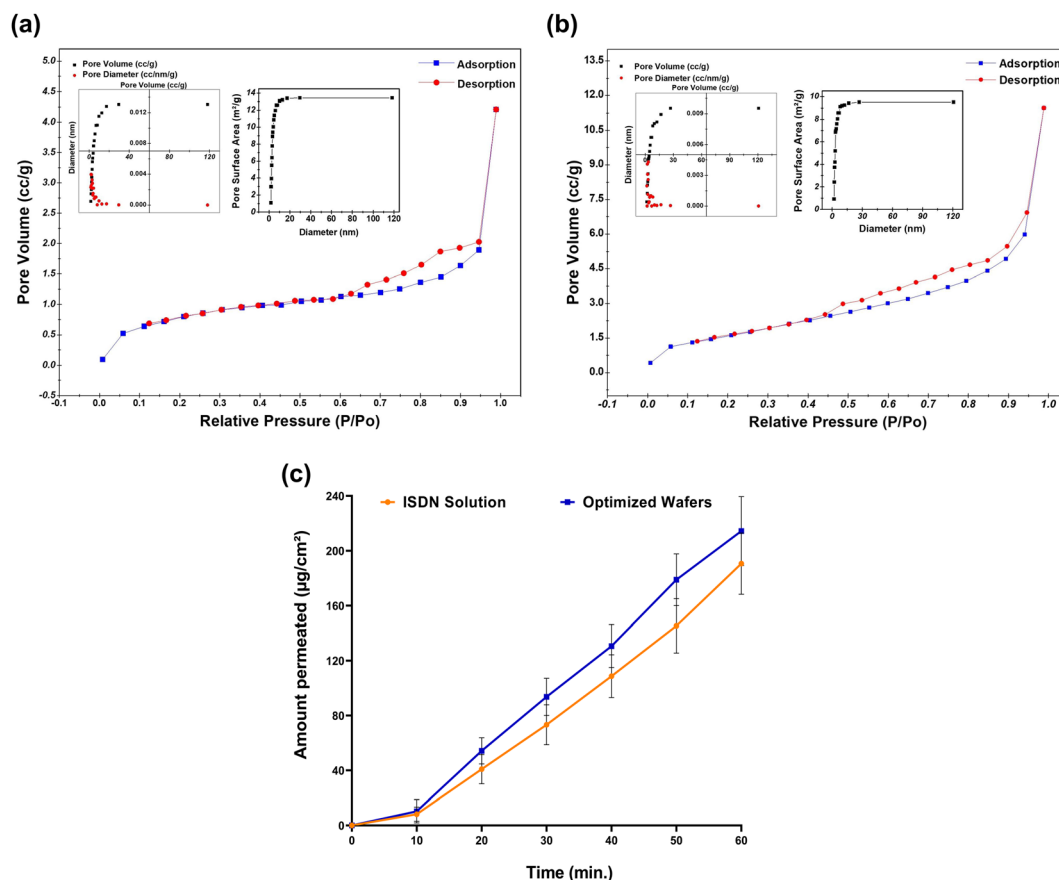
ted sub-micron pores throughout the hydrophilic wafer matrix. These pores facilitate rapid fluid penetration, significantly reducing DT by enabling quick fluid uptake. This porous architecture promotes the wafer's rapid breakdown upon contact with saliva, likely resulting in pulsatile drug release. Such burst release may enhance absorption and induce a timely onset of therapeutic action.[44]

AFM is a useful tool to evaluate the suitability of wafers for transmucosal application.[45] AFM was utilized to analyze the three-dimensional structure and surface roughness at small and large scales. The surface roughness values of R_a, R_q, and R_z were found to be 0.75, 0.99, and 11.6 nm, respectively, indicating a highly smooth surface with minimal irregularities. These findings were further confirmed by 3D surface morphology images obtained from AFM (Fig. 8c). The AFM images indicated the suitability of wafers for sublingual or transmucosal application.

Structural characterisation. The nitrogen adsorption–desorption isotherms of both wafer and film formulations revealed a type IV pattern with H3 hysteresis loops, indicating the presence of mesoporous structures. The nitrogen sorption data for wafers and films are presented. The film exhibited a specific surface area of 9.523 m^2 g^{-1} with an average pore diameter of 3.343 nm and total pore volume of ~0.010 cm^3 g^{-1}, reflecting a denser and more compact structure (Fig. 9a). In contrast, the wafer displayed a specific surface area of 13.428 m^2 g^{-1} and pore diameter of ~2.039 nm, with relatively higher pore volume (~0.013 cc g^{-1}), indicating a relatively porous matrix that could initiate a rapid release (Fig. 9b). The higher surface area and pore volume in the wafer compared to the film can be attributed to the preservation of mesopores and the formation of voids during the lyophilisation, as corroborated by SEM evidence.[24] Density analysis further supported these findings, as the density of the films (1.44 ± 0.23 g cm^{-3}) was found to be significantly higher ($p < 0.04$) than that of the wafers (0.633 ± 0.012 g cm^{-3}), further confirming the denser structure of films and the porous nature of wafers. The film, prepared by SC, transforms into a dense three-dimensional cross-linked network with reduced porosity, which accounts for its lower pore volume. In contrast, the wafer produced by lyophilisation exhibits a more relaxed polymer alignment with greater structural flexibility, enabling significant pore expansion during the drying process.

***Ex vivo* permeation.** *Ex vivo* permeation studies using porcine buccal mucosa showed that ISDN sublingual wafers displayed a steady-state flux of 3.77 ± 1.58 µg cm^{-2} min^{-1},

Fig. 9 Nitrogen adsorption–desorption isotherms and corresponding Barrett–Joyner–Halenda (BJH) pore size distribution curves of (a) film and (b) wafer formulation. (c) *Ex vivo* permeation data of the optimised batch and drug solution at 37 ± 2 °C. Data are presented as mean $\pm$ S.D. (n = 3).
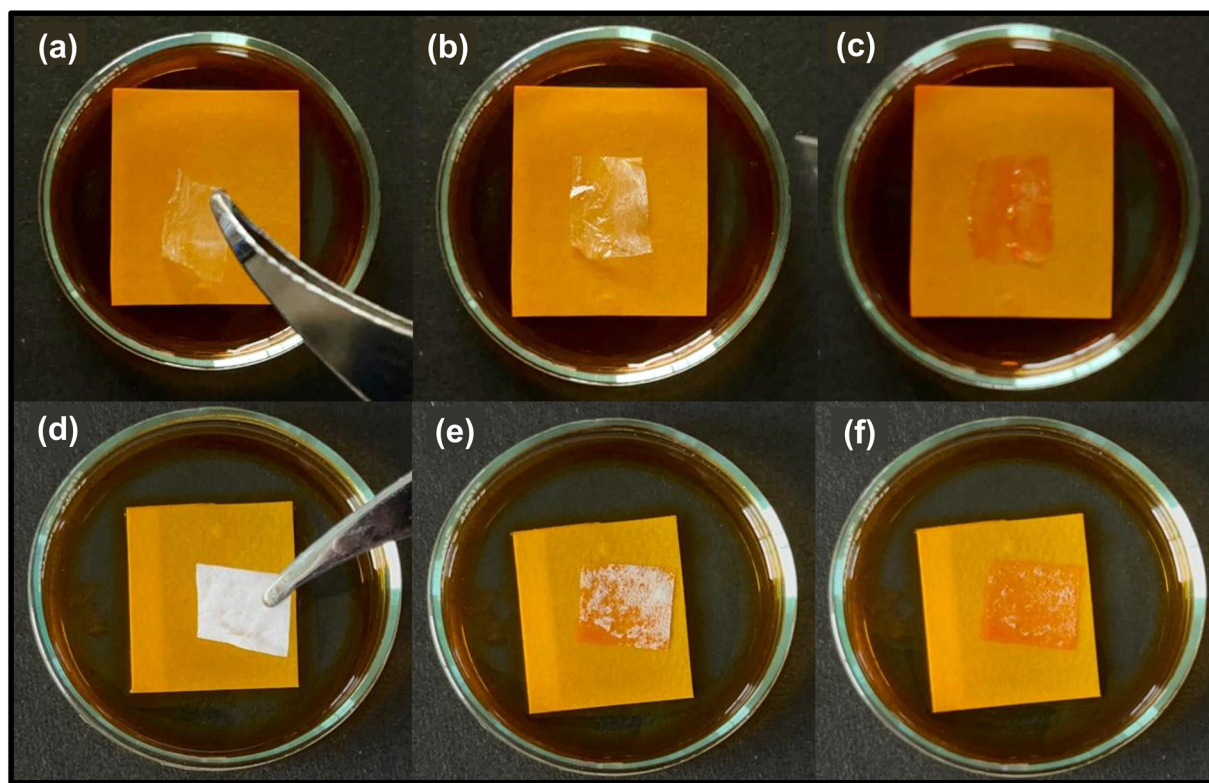
Fig. 10 Visual representation of the wetting time of the developed sublingual (a–c) film and (d–f) wafers.

Table 6 The mean values of folding endurance, moisture loss, disintegration time, and drug content of optimised isosorbide dinitrate-loaded sublingual wafers at the end of 3 months at room temperature

Storage interval (days)	FE[a]	Moisture loss (%)	DT[b] (s)	DC[c] (%)
0	280 ± 2	0.53 ± 0.07	2.58 ± 0.1	99.73 ± 1.63
30	280 ± 5	0.53 ± 0.01	2.58 ± 0.5	99.72 ± 1.62
60	278 ± 1	0.52 ± 0.04	2.60 ± 0.2	99.69 ± 1.53
90	274 ± 2	0.51 ± 0.02	2.64 ± 0.1	98.76 ± 1.48

*All data are expressed as mean ± SD ($n = 3$). [a] Folding endurance. [b] Disintegration time. [c] Drug content.

which was found to be comparable ($p > 0.05$) to the flux from ISDN solution (3.26 ± 1.41 μg cm^{-2} min^{-1}). These findings indicate that the wafer formulation can facilitate ISDN permeation more efficiently compared to the solution. The results, depicted in Fig. 9c, highlight the robust performance of the sublingual wafer in delivering the drug through the mucosal membrane. Notably, these wafers are expected to rapidly disperse in the sublingual cavity, enabling quick drug release. The soluble form of the drug in the sublingual cavity is likely to be quickly absorbed to offer timely protection against cardiovascular risks. In addition, by virtue of the ability to bypass first-pass hepatic metabolism, the wafers are likely to improve the systemic availability of ISDN. Overall, the

study supports sublingual wafer delivery as a promising approach for rapid and effective ISDN administration.

Wetting time. A simulated wetting test was performed to determine the water absorption time. Studies indicated that wetting correlated well with DT. Wetting time was found to be 20.3 ± 0.3 s for films, as depicted in Fig. 10(a–c), which was found to be significantly higher ($p < 0.0001$) compared to that of the lyophilised wafers, which was found to be 2.1 ± 0.5 s as illustrated in Fig. 10(d–f). The shorter wetting time can be attributed to quick diffusion and water intake into the porous microchannels of the wafers.[46] The better wettability can be ascribed to the porous microstructure of the hydrophilic matrix of the wafers developed by lyophilisation. Shorter wetting time would result in quicker disintegration, which in turn would hasten the *in vitro* dissolution.[47] This rapid disintegration is primarily due to improved capillary action and the wafer's capability to absorb and distribute the medium throughout its structure effectively. These observations highlight the importance of optimising wetting time when designing formulations that need rapid disintegration, as it determines their overall performance and effectiveness.[48]

Stability studies. The optimised sublingual ISDN wafers maintained stable physical and chemical properties during 90 days of storage at room temperature. No significant changes were observed in FE, moisture loss, DT, and DC, and all measured parameters were not statistically significant ($p > 0.05$), as depicted in Table 6. These results indicate that the

formulation is stable and suitable for long-term storage without loss of quality or performance.

Conclusions

Fast-dissolving polymeric wafers of isosorbide dinitrate were successfully developed by optimising lyophilisation process parameters, including the drying surface area and volume of the casting solution. The sublingual wafers, produced by freeze-drying, exhibited the most desirable critical quality attributes, including rapid disintegration and quick dissolution. The porous microstructure of the wafers and the amorphous nature of the drug in the hydrophilic polymeric matrix were found to be crucial in facilitating rapid fluid uptake, which resulted in faster disintegration and generated a pulsed drug release. The polymeric wafers will instantaneously dissolve in the sublingual cavity, and thus are likely to elicit rapid onset, minimising ischemic damage during cardiac distress when patients might lose consciousness. Moreover, the developed wafers will overcome the challenges associated with oral administration, such as poor bioavailability due to first-pass metabolism. The platform technology that can be deployed in emergency medicine is likely to induce a paradigm shift in the prophylactic management of cardiac emergencies such as angina. Future studies need to focus on scale-up and large-scale production, followed by validation of the promising technology for wider clinical applications.

Author contributions

Megha Kamath: writing – original draft, methodology, investigation, formal analysis. Avichal Kumar, Sanjana S.P., Raksha Pai and Rushikesh Shinde: writing – review & editing, formal analysis, data curation, and software. Shivakumar H. N. and Vanita Somasekhar: writing – review & editing, methodology, investigation, and conceptualisation.

Conflicts of interest

There are no conflicts to declare.

Data availability

All data analysed or generated during this study are included in this article.

Acknowledgements

References

1 M. A. B. Khan, M. J. Hashim, H. Mustafa, *et al.*, Epidemiology of type 2 diabetes – global burden of disease and forecasted trends, *Cureus*, 2020, **12**(7), e9349.

2 S. Steven, M. Oelze, M. Hausding, *et al.*, The endothelin receptor antagonist macitentan improves isosorbide-5-mononitrate (ISMN) and isosorbide dinitrate (ISDN) induced endothelial dysfunction, oxidative stress, and vascular inflammation, *Oxid. Med. Cell. Longevity*, 2018, **2018**, 1–17.

3 K. C. Ferdinand, U. Elkayam, D. Mancini, *et al.*, Use of isosorbide dinitrate and hydralazine in African-Americans with heart failure 9 years after the African-American heart failure trial, *Am. J. Cardiol.*, 2014, **114**(1), 151–159.

4 K. El Refaie, A. M. Abd, El, Hay, N. Saad, M. M. Azaam and K. R. Shoueir, Synthesis and characterization of poly(+) lactic acid and its application as sustained release of isosorbide dinitrate, *Sci. Rep.*, 2024, **14**, 7062.

5 H. Y. Cao, H. D. Wu, Z. K. Song, *et al.*, Higher than recommended dosage of sublingual isosorbide dinitrate for treating angina pectoris: a case report and review of literature, *Pan Afr. Med. J.*, 2021, **39**(28), DOI: 10.11604/pamj.2021.39.28.22180.

6 M. Alami-Milani, S. Salatin, E. Nasiri and M. Jelvehgari, Preparation and optimization of fast disintegrating tablets of isosorbide dinitrate using lyophilisation method for oral drug delivery, *Ther. Delivery*, 2021, **12**(7), 523–538.

7 L. L. Silva, M. D. Duque, M. G. Issa and L. N. C. Rodrigues, Isosorbide orally disintegrating films cyclodextrin/HPMC based: mechanical, optical and physicochemical studies, *Braz. Arch. Biol. Technol.*, 2023, **66**, e23220370.

8 M. Fathi, M. Alami-Milani, S. Salatin, *et al.*, Fast dissolving sublingual strips: a novel approach for delivery of isosorbide dinitrate, *Pharm. Sci.*, 2019, **25**(4), 311–318.

9 S. H. Jeong, Y. Fu and K. Park, FrostaR: a new technology for making fast-melting tablets, *Expert Opin. Drug Delivery*, 2005, **2**(6), 1107–1116.

10 J. S. Costa, C. K. de Oliveira and L. Oliveira-Nascimento, A minireview on drug delivery through wafer technology: formulation and manufacturing of buccal and oral lyophilizates, *J. Adv. Res.*, 2019, **20**, 33–41.

11 K. Chougule, P. M. Dandagi and S. Hulyalkar, Esomeprazole-loaded flash release sublingual wafers: formulation, optimization, and characterization, *J. Pharm. Innov.*, 2023, **18**(4), 2013–2028.

12 M. H. Siddiqui, M. S. Islam, M. R. Razu, *et al.*, Preparation and evaluation of sublingual film of ketorolac tromethamine, *Drug Dev. Ind. Pharm.*, 2022, **48**, 438–445.

13 K. Joshi, U. V. Bhandarkar and S. S. Joshi, Surface integrity and wafer-thickness variation analysis of ultra-thin silicon wafers sliced using wire-EDM, *Adv. Mater. Processes Technol.*, 2019, **5**(3), 512–525.

14 M. Maghsoodi, M. Rahmani, H. Ghavimi, *et al.*, Fast dissolving sublingual films containing sumatriptan alone and combined with methoclopramide: evaluation in vitro drug release and mucosal permeation, *Pharm. Sci.*, 2016, **22**, 153–163.

15 A. Chandra, A. D. Chondkar, R. Shirodkar and S. A. Lewis, Rapidly dissolving lacidipine nanoparticle strips for transbuccal administration, *J. Drug Delivery Sci. Technol.*, 2018, **47**, 259–267.

16 M. Fathei, M. Alami-Milani, S. Salatin, *et al.*, Fast dissolving sublingual strips: a novel approach for the delivery of isosorbide dinitrate, *Pharm. Sci.*, 2019, **25**(4), 311–318.

17 S.-F. Ng and N. Jumaat, Carboxymethyl cellulose wafers containing antimicrobials: a modern drug delivery system for wound infections, *Eur. J. Pharm. Sci.*, 2014, **51**, 173–179.

18 M. N. Pham, T. Van Vo, V.-T. Tran, P. H.-L. Tran and T. T.-D. Tran, Microemulsion-based mucoadhesive buccal wafers: wafer formation, in vitro release, and ex vivo evaluation, *AAPS PharmSciTech*, 2017, **18**(7), 2727–2736.

19 M. K. Raval, J. M. Patel, R. K. Parikh and N. R. Sheth, Studies on influence of polymers and excipients on crystallization behavior of metformin HCl to improve the manufacturability, *Part. Sci. Technol.*, 2017, **32**, 431–444.

20 D. Avlani, A. Kumar and H. N. Shivakumar, Development of dispersible vaginal tablets of tenofovir loaded mucoadhesive chitosan microparticles for anti-HIV pre-exposure prophylaxis, *Mol. Pharm.*, 2023, **20**(10), 5006–5018.

21 V. A. Echanur, A. V. Matadh, S. G. Pragathi, *et al.*, Continuous manufacturing of oil-in-water (O/W) emulgel by extrusion process, *AAPS PharmSciTech*, 2023, **24**, 76.

22 L. Gallo, M. V. Ramírez-Rigo and V. Bucalá, Development of porous spray-dried inhalable particles using an organic solvent-free technique, *Powder Technol.*, 2019, **342**, 642–652.

23 V. A. Lapitskaya, T. A. Kuznetsova, A. V. Khabarava, *et al.*, The use of AFM in assessing the crack resistance of silicon wafers of various orientations, *Eng. Fract. Mech.*, 2022, **259**, 107926.

24 M. Guo, X. Zou, H. Ren, *et al.*, Fabrication of high surface area mesoporous silicon via magnesiothermic reduction for drug delivery, *Microporous Mesoporous Mater.*, 2011, **142**(1), 194–201.

25 A. Dinge and M. Nagarsenker, Formulation and evaluation of fast dissolving films for delivery of triclosan to the oral cavity, *AAPS PharmSciTech*, 2008, **9**(2), 349–356.

26 P. Hooper, J. Lasher, K. S. Alexander and G. Baki, A new modified wetting test and an alternative disintegration test for orally disintegrating tablets, *J. Pharm. Biomed. Anal.*, 2016, **120**, 391–396.

27 S. S. Timur, S. Yüksel, G. Akca and S. Şenel, Localized drug delivery with mono and bilayered mucoadhesive films and wafers for oral mucosal infections, *Int. J. Pharm.*, 2019, **559**, 102–112.

28 J. C. Kasper, G. Winter and W. Friess, Recent advances and further challenges in lyophilisation, *Eur. J. Pharm. Biopharm.*, 2013, **85**(2), 162–169.

29 I. Ayensu, J. C. Mitchell and J. S. Boateng, Development and physico-mechanical characterisation of lyophilised chitosan wafers as potential protein drug delivery systems via the buccal mucosa, *Colloids Surf., B*, 2012, **91**, 258–265.

30 P. Fonte, S. Reis and B. Sarmento, Facts and evidences on the lyophilisation of polymeric nanoparticles for drug delivery, *J. Controlled Release*, 2016, **225**, 75–86.

31 K. Korelc, B. S. Larsen, M. Gašperlin and I. Tho, Water-soluble chitosan eases development of mucoadhesive buccal films and wafers for children, *Int. J. Pharm.*, 2023, **631**, 122544.

32 C. Woertz and P. Kleinebudde, Development of orodispersible polymer films containing poorly water soluble active pharmaceutical ingredients with focus on different drug loadings and storage stability, *Int. J. Pharm.*, 2015, **493**(1–2), 134–145.

33 Y. Alhamhoom, A. K. Said, A. Kumar, S. H. Nanjappa, D. Wali, M. Rahamathulla, *et al.*, Sublingual fast-dissolving thin films of loratadine: Characterization, in vitro and ex vivo evaluation, *Polymers*, 2024, **16**(20), 2919.

34 A. Berardi, P. H. M. Janssen and B. H. J. Dickhoff, Technical insight into potential functional-related characteristics (FRCs) of sodium starch glycolate, croscarmellose sodium and crospovidone, *J. Drug Delivery Sci. Technol.*, 2022, **70**, 103261.

35 S. H. Hong, Y. Cho and S. W. Kang, Formation of water-channel by propylene glycol into polymer for porous materials, *Membranes*, 2021, **11**(11), 881.

36 M. Chen, W. Zhang, H. Wu, C. Guang and W. Mu, Mannitol: physiological functionalities, determination methods, biotechnological production, and applications, *Appl. Microbiol. Biotechnol.*, 2020, **104**(16), 6941–6951.

37 M. Manyikana, Y. E. Choonara, L. K. Tomar, C. Tyagi, P. Kumar, L. C. du Toit, *et al.*, A review of formulation techniques that impact the disintegration and mechanical properties of orodispersible drug delivery technologies, *Pharm. Dev. Technol.*, 2016, **21**(3), 354–366.

38 M. G. A. Vieira, M. A. da Silva, L. O. dos Santos and M. M. Beppu, Natural-based plasticizers and biopolymer films: A review, *Eur. Polym. J.*, 2011, **47**(3), 254–263.

39 R. N. Wadetwar, F. Ali and P. R. Kanojiya, Formulation and evaluation of fast dissolving sublingual film of paroxetine hydrochloride for treatment of depression, *Asian J. Pharm. Clin. Res.*, 2019, **12**, 126–132.

40 J. Chen, Food oral processing: Mechanisms and implications of food oral destruction, *Trends Food Sci. Technol.*, 2015, **45**(2), 222–228.

41 D. Markl and J. A. Zeitler, A review of disintegration mechanisms and measurement techniques, *Pharm. Res.*, 2017, **34**(5), 890–917.

42 J. U. Maheswari, S. Muthu and T. Sundius, An experimental and theoretical study of the vibrational spectra and structure of isosorbide dinitrate, *Spectrochim. Acta, Part A*, 2013, **109**, 322–330.

43 K. Zao, T. Ishiguro, D. Iohara, M. Anraku, H. Seo, T. Irie, *et al.*, In vitro transdermal permeation behavior of isosorbide dinitrate in the absence and presence of 2-hydroxypropyl-β-cyclodextrin: solutions and suspensions, *J. Inclusion Phenom. Macrocyclic Chem.*, 2020, **96**(1–2), 137–143.

44 R. Sharma, S. Kamboj, G. Singh and V. Rana, Development of aprepitant loaded orally disintegrating films for enhanced pharmacokinetic performance, *Eur. J. Pharm. Sci.*, 2016, **84**, 55–69.

45 J. S. Boateng, A. D. Auffret, K. H. Matthews, M. J. Humphrey, H. N. E. Stevens and G. M. Eccleston, Characterisation of freeze-dried wafers and solvent evapor-ated films as potential drug delivery systems to mucosal surfaces, *Int. J. Pharm.*, 2010, **389**(1–2), 24–31.

46 H. Wei, X. Sha, L. Chen, Z. Wang, C. Zhang, P. He, *et al.*, Visualization of multiphase reactive flow and mass transfer in functionalized microfluidic porous media, *Small*, 2024, **20**(32), e2401393.

47 N. Zaborenko, Z. Shi, C. C. Corredor, B. M. Smith-Goettler, L. Zhang, A. Hermans, *et al.*, First-principles and empirical approaches to predicting in vitro dissolution for pharmaceutical formulation and process development and for product release testing, *AAPS J.*, 2019, **21**(3), 32.

48 Y. Alhamhoom, T. Kumaraswamy, A. Kumar, S. H. Nanjappa, S. S. Prakash, M. Rahamathulla, *et al.*, Formulation and evaluation of pH-modulated amorphous solid dispersion-based orodispersible tablets of cefdinir, *Pharmaceutics*, 2024, **16**(7), 866.